{ TC "'CHAPTER FIVE: MODEL CONSTRUCTION AND VERIFICATION':" \l 1 \n }CHAPTER

FIVE

MODEL CONSTRUCTION AND VERIFICATION

5.1 Introduction{ TC "5.1 Introduction" \l 2 }

In the last chapter, the necessary component models to be used with the TRNSYS program for simulating photovoltaic-powered solar domestic hot water (PV-SDHW) systems were introduced and described. These components were assembled to form a TRNSYS model of a two-tank PV-SDHW system. For purposes of verifying the accuracy of this model, experimental data were obtained from two prototype installations. The first, located at the National Institute of Standards and Technology (NIST) in Gaithersburg, MD became operational in July, 1995. The period of July 1, 1995 through June 30, 1996 was simulated using the TRNSYS model. The second prototype, located at the Florida Solar Energy Center (FSEC), became operational in December, 1995. This system was simulated for the period of December 23, 1995 through September 26, 1996.

5.2 The Prototype Systems{ TC "5.2 The Prototype Systems" \l 2 }

5.2.1 System Descriptions{ TC "5.2.1 System Descriptions" \l 3 }

Table 5.2.1-1 presents the specifications for the two prototype systems. Both systems used PV modules manufactured by Siemens (model M55) and water tanks by A.O. Smith (models PEC-80 and PEH-52 for the preheat and auxiliary tanks, respectively).

Table 5.2.1-1 System specifications for the two prototypes modeled in this analysis.**{** TC **"Table 5.2.1-1** System specifications for the two prototypes modeled in this analysis.**" \l 6 }**

	NIST Prototype System II	**FSEC System**
Location	Gaithersburg, MD	Cocoa, FL
Latitude	39.2 N	28.4 N
Photovoltaic Array Size (m^2)	12.80	11.52
Array Slope	40	24
Number of Modules in Series	10	9
Number of Module Strings in Parallel	3	3
Nominal/Actual Preheat Tank Volume (L)	303 / 272.4	303 / 272.4
Nominal/Actual Auxiliary Tank Volume (L)	190 / 170.4	190 / 170.4
Auxiliary Tank Thermostat Setpoint (C)	57.0	51.7
Preheat Tank Heat Loss Coefficient (W/ C)	1.92	2.17
Auxiliary Tank Heat Loss Coefficient (W/ C)	1.21	1.43
Preheat Tank Upper Heating Elements (Nominal Resistance ( ) - Operating Sequence)	180 - 1 120 - 5 75 - 6	120 - 1 120 - 5 120 - 6
Preheat Tank Lower Heating Elements (Nominal Resistance ( ) - Operating Sequence)	180 - 2 110 - 3 75 - 4	90 - 2 90 - 3 110 - 4
Solar Irradiance Range, G_T (W/m^2), for Each Nominal Resistive Load ( )	180: $5 < G_T$ 138 90: $138 < G_T$ 273 50: $273 < G_T$ 483 30: $483 < G_T$ 687 24: $687 < G_T$ 882 18: $882 < G_T$	120: 18 $G_T < 200$ 51: 200 $G_T < 385$ 33: 385 $G_T < 540$ 26: 540 $G_T < 675$ 21: 675 $G_T < 800$ 18: 800 G_T

The resistor switching controller in the NIST and FSEC installations used a reference PV cell to provide the irradiance measurement for control. In this device, the cell's short circuit current is measured and correlated with radiation intensity. Irradiation was also independently recorded using a calibrated pyranometer. The control logic in the NIST prototype was designed to make a resistor switching decision every 20 seconds based on an instantaneous irradiance reading. The

FSEC system, on the other hand, allowed switching every 60 seconds based on the average of three irradiance readings (taken every 20 seconds).

5.2.2 Available Data{ TC "5.2.2 Available Data" \l 3 }

Both of the prototype installations were instrumented to record all pertinent measurements in order to assess the performance of these systems and to provide data for model validation. Shown in Table 5.2.2-1 is a list of the data which were available from these two sites in hourly intervals.

Table 5.2.2-1 Data available from NIST and FSEC prototype operation on an hourly basis.**{** TC "**Table 5.2.2-1** Data available from NIST and FSEC prototype operation on an hourly basis." **\l 6 }**

energy removed from preheat tank as a result of draws (kJ)
energy removed from auxiliary tank as a result of draws (kJ)
energy removed from total system as a result of draws (kJ)
average inlet temperature of preheat tank (C)
average outlet temperature of preheat tank (C)
average inlet temperature of auxiliary tank (C)
average outlet temperature of auxiliary tank (C)
electrical energy supplied by PV panels (kJ)
electrical energy supplied to auxiliary tank (kJ)
total heat loss from preheat tank (kJ)
total heat loss from auxiliary tank (kJ)
mass of water removed from system (kg)
solar energy received by PV array as measured by pyranometer (kJ/m^2)
solar energy received by PV array as measured by reference PV cell (kJ/m^2)*
average outdoor temperature (C)
average PV panel temperature (C)
average indoor temperature (C)
average water temperature in preheat tank (C)
average water temperature in auxiliary tank (C)

* these hourly data only provided for FSEC system

In addition to the above hourly data, data were available on a minutely basis from the NIST prototype only. These minutely data included the six internal temperature measurements made in each tank to estimate the average tank temperature. The locations of these measurements were at the center of six equal volume segments along the height of the tank.

The use of the supplied hourly data was complicated by the fact that it contained some gaps lasting from a few hours to several days. These gaps resulted from temporary shutdowns of all or part of the system due to malfunction, for repair, or because of snow cover on the array and/or irradiation sensor. The FSEC system, for example, was shut down during April 12-18, 1996 as a result of a leaking auxiliary tank. The problem was solved by replacing the tank. A measured data set for use in model validation for each prototype was constructed according to the following rules: only hourly data from days containing no anomalies of any kind were included and "good" operational periods less than two days in length were excluded (Dougherty, 1996). As a result, the simulation of the NIST prototype was run in 21 separate time segments and the FSEC simulation in four segments. The discontinuous nature of the resulting simulations necessitated the use of initial tank temperature distributions for each data time period. In the case of the NIST model, this information was provided to TRNSYS using the NIST-measured tank temperature distributions for the first minute of each period. Thus TRNSYS began each simulation period with exactly the measured temperatures for each of the six temperature nodes in the tanks. In modeling the FSEC system, in the absence of minutely data, the initial tank temperatures for each period were taken as the average tank temperatures for the first hour of the period. Initial tank temperature distributions were unavailable and uniform average temperatures had to suffice as initial conditions for the TRNSYS tank models. The effect on the average tank temperature of using average tank temperature initial conditions rather than tank temperature distribution initial conditions was

determined by simulation to disappear after the first 24-36 hours of a simulation period. The use of average tank temperature as the initial condition in the FSEC simulation was assumed to have a negligible effect on long term results.

5.3 Modeling the Tanks{ TC "5.3 Modeling the Tanks" \l 2 }

The preheat and auxiliary water storage tanks were simulated using the TRNSYS tank model discussed in the last chapter. The tank volumes were set as the actual volumes measured on the prototype tanks. The tank heights were set as recommended by Dougherty (1995) and were slightly lower than the actual outside tank dimensions given by the manufacturer. The tanks were divided into 18 volume segments by the tank model. Inlet water to each tank was assumed to enter the node closest to it in temperature (virtually always the bottom segment). Outlet streams from the tanks were taken from the very top of the tanks as occurs in practice. Water was assumed to have a constant specific heat of 4.18 kJ/kg K, a constant thermal conductivity of 0.64 W/m K, and a constant density of 1000 kg/m^3 for the temperatures encountered in this application.

The overall heat loss coefficients, U, for the preheat and auxiliary tanks were determined for purposes of modeling the NIST and FSEC systems by simulating the cooldown tests of the tanks which established their UA values in practice. In these simulations, the tanks had surface areas consistent with the actual estimated tank dimensions from Dougherty (1996). Each tank was initially at a uniform elevated temperature of 75 C with a constant ambient air temperature of 25 C. The value of UA, virtually constant with time, was plotted as the simulation progressed to observe its value. The value of U for each tank was adjusted such that during the cooldown simulation the simulated UA was nearly equal to the UA measured from the prototype systems. UA was defined as

$$UA = \frac{q_{loss}}{(T_{tank,avg} - T_a)} \qquad (5.3.1)$$

where q_{loss} is the rate of heat loss from the tank, $T_{tank,avg}$ is the average temperature of the water in the tank, and T_a is the ambient air temperature. The indoor ambient air temperature for the later prototype simulations was taken to be equal to that measured at the prototype installations.

The PV-connected heating elements in the preheat tank were allowed to heat the water whenever power was available. The heating elements in the auxiliary tank were controlled in a master/slave relationship in which the bottom element could be energized only when the top element was satisfied. The elements could not operate simultaneously. The positions of the heating elements and thermostats (in the auxiliary tank) were set according to the advice of Dougherty (1996). The thermostat setpoints and temperature deadbands were adjusted by trial and error such that the outlet water temperature and average tank water temperature temporal profiles for the auxiliary tank were nearly the same as those measured from the prototypes. The upper and lower thermostat set points and deadbands were assumed equal and the heating rates of the auxiliary elements were set to 4.5 kW like the prototype systems.

Possible heat losses from the pipe joining the preheat and auxiliary tanks were accounted for by use of a TRNSYS component model of a pipe. This model simulates the thermal behavior of fluid flow in a pipe using variable size segments of fluid in "plug-flow." It does not consider mixing or conduction between adjacent fluid elements. The overall heat loss coefficient for the pipe was estimated by analytical means based on the known pipe and insulation materials and dimensions.

5.4 Modeling the Photovoltaic Array, Resistors, and Controller{ TC "5.4 Modeling the Photovoltaic Array, Resistors, and Controller" \l 2 }

The PV array was simulated using the model discussed in the last chapter. The parameters describing the array were set according to values measured independently by Fanney and Dougherty at NIST (Dougherty, 1996). Data regarding the array dimensions was taken from the Siemens literature. Table 5.4-1 presents the PV parameters supplied by NIST and those given in

the Siemens literature.

Table 5.4-1 Siemens M55 PV module reference performance parameters as presented by manufacturer and from independent measurements by NIST.**{** TC **"Table 5.4-1** Siemens M55 PV module reference performance parameters as presented by manufacturer and from independent measurements by NIST.**" \l 6 }**

Module Characteristic	**Siemens**	**NIST**
$G_{T,ref}$	1000 W/m^2	904.8 W/m^2
$T_{c,ref}$	25 C	45.3 C
$I_{sc,ref}$	3.4 A	3.056 A
$V_{oc,ref}$	21.7 V	19.951 V
$I_{mp,ref}$	3.05 A	2.781 A
$V_{mp,ref}$	17.4 V	15.248 V
$\mu_{I,sc}$	0.00 A/ C	0.001818 A/ C
$\mu_{V,oc}$	-0.12 V/ C	-0.07561 V/ C

Using the NIST-measured parameters in the TRNSYS array model and simulating the standard reference conditions used by Siemens in establishing the values indicated that the NIST parameters produce a maximum power about 3% less than that suggested by Siemens. A constant heat loss coefficient U_L for the PV array was estimated using the nominal operating cell temperature (NOCT) reported in the Siemens literature. The NOCT is defined as the module temperature reached when the solar radiation on the cells is 800 W/m^2, the wind speed is 1 m/s , and the ambient temperature is 20 C. Siemens reported the NOCT for the M55 to be 42 C ± 2 C. Using this information in Equation 4.4.12 with $\tau\alpha$ assumed 0.9 and $\eta_c/\tau\alpha$ small relative to unity yields a U_L of 32.7 W/m^2 C. Outdoor ambient temperatures used in the simulations were taken as those measured at the prototype installations.

Irradiation data from the pyranometer was input to the TRNSYS PV array component. In hourly simulations of the FSEC system and minutely simulations of the NIST system, irradiation data

from the PV reference cell was input to the switching controller model. In the NIST hourly simulations, however, the pyranometer irradiation was input to the controller as the reference cell data was not available on an hourly basis. In the long-term hourly simulations, the TRNSYS model considered switching between resistive loads only once each hour as new irradiance values were available. The constant irradiation level for each hour (in kJ/hr-m^2) was taken to be equal in magnitude to the reported total irradiation for the hour (in kJ/m^2). Using hourly and minutely data for an identical time period, an assessment was made of the difference in model performance resulting from the use of a constant, average hourly irradiation rate with a constant resistive load and the use of minute-by-minute irradiation rates and resistive load changes. Hourly and minutely data from nine days between May 15, 1996 and May 23, 1996 for the NIST prototype were used in two simulations. The resulting total PV array energy outputs for the nine day period using hourly and minutely simulations differed by approximately 0.5 %.

The multiple resistive elements and the switching controller were modeled using the TRNSYS component discussed in the last chapter. The values of the resistors were taken as the nominal values reported by Fanney and Dougherty (1996) for the NIST and FSEC prototypes. The order of resistor connection and the irradiance levels at which switches were initiated were also taken directly as those used in the prototypes .

5.5 Modeling the Hot Water Draws{ TC "5.5 Modeling the Hot Water Draws" \l 2 }

Proper draws of hot water from the auxiliary tank were simulated directly from the measured draw masses. In the prototypes, the water draw flow rate was approximately 3 gpm and the draws were initiated at the beginning of the hour in which they took place. The hot water draw profile imposed on the prototypes consisted of draws of 20.5 L, 61.0 L, and 40.5 L occurring at 6 AM, 7 AM, and 8 AM, respectively, and repeating at 6 PM, 7 PM, and 8 PM. In the hourly simulations, since only hourly water draw masses were known, the draws were assumed to occur

during the first four minutes of all draw hours. The actual hourly draws of approximately 20.5 L, 61.0 L, and 40.5 L required approximately 1.8 minutes, 5.4 min, and 3.6 min, respectively. In minutely simulations of the NIST prototype, no water draw data were available on a minutely basis and the draws were assumed to be exactly 20.5 L, 61.0 L, and 40.5 L and to occur in 2 minutes, 5 minutes, and 4 minutes, respectively. The simulated cold inlet water temperature to the preheat tank was equal to that measured in the prototype operation.

5.6 Modeling the NIST Prototype{ TC "5.6 Modeling the NIST Prototype" \l 2 }

The model described above was used first to simulate the performance of the prototype at NIST. This was the first prototype to begin operation and more detailed data was available for it (minutely) than for the FSEC system.

5.6.1 Experimental Measurements{ TC "5.6.1 Experimental Measurements" \l 3 }

Table 5.6.1-1 shows measured monthly and overall results for the NIST system for the twelve months of data used for verification purposes. Individual tank and overall system loads were defined as

$$\text{load} = \int_{\text{time}} \dot{m} c_p (T_{out} - T_{in}) \, \text{dtime} \qquad (5.6.1.1)$$

where $\dot{m}$ is the water mass flow rate, c_p is the water specific heat, T_{out} is the water temperature exiting the tank or system, and T_{in} is the water temperature entering the tank or system. Tank heat losses were defined as

$$\text{loss} = \int_{\text{time}} UA (T_{tank} - T_{amb}) \, \text{dtime} \qquad (5.6.1.2)$$

where UA is the overall heat loss coefficient for the tank, T_{tank} is the average water temperature in

the tank, and T_{amb} is the ambient air temperature. The solar fraction figures refer to the preheat tank load divided by the total system load. The tank "Delta Energy" values refer to the change in tank internal energy as measured by the average tank temperatures for the first and last hours of the given period. The tank "Data Gap Energy" quantifies the internal energy added to the tank during periods of missing data as calculated from the average tank temperatures for the hours immediately before and after the gaps. The tank "Energy Unbalance" figures represent the sum of the tank load, heat loss, and change in internal energy subtracted from the sum of the tank electrical input and data gap energy addition. The Overall "Energy Unbalance" figures are the sum of the two tank unbalances. The experimental results in Table 5.6.1-1 will be discussed and compared with the results of the TRNSYS simulation of the NIST system in the following sections.

Table 5.6.1-1 NIST performance results for the period July 1, 1995 through June 30, 1996.**{** TC **"Table 5.6.1-1** NIST performance results for the period July 1, 1995 through June 30, 1996." **\l 6 }**

Month	Jul	Aug	Sep	Oct	Nov	Dec	Jan	Feb	Mar	Apr	May	Jun	Total
Preheat Tank Load (kJ)	721417	802220	618818	797201	476559	518014	254141	443068	548316	618223	661857	790752	7250586
Auxiliary Tank Load (kJ)	508087	523614	568363	618039	825979	717702	571464	605080	482934	532474	759580	567432	7280748
Total Load (kJ)	1216390	1309738	1171316	1395462	1286759	1236376	828864	1052836	1035399	1151170	1407585	1344692	14436587
Preheat Tank Heat Loss (kJ)	27648	29635	16051	25018	-5510	3550	-8320	1674	10844	12582	4667	22627	140466
Auxiliary Tank Heat Loss (kJ)	93405	99735	88963	106264	95895	90193	61754	79093	79159	88952	105768	102509	1091688
Water Draw (kg)	6492	6971	6253	7462	6741	6400	4330	5537	5541	6265	7469	7229	76691
Preheat Tank Electrical Input (kJ)	736341	817319	638694	793635	469730	524595	253948	482448	633201	653980	675121	801966	7480977
Auxiliary Tank Electrical Input (kJ)	604446	623398	660984	731053	932237	811396	639554	688568	565699	626937	869043	668160	8421476
Preheat Tank Average Temp. (C)	30.0	30.0	27.6	28.8	22.7	24.3	20.9	24.3	26.7	26.8	24.9	28.4	26.5
Auxiliary Tank Average Temp. (C)	56.9	56.8	56.6	56.7	56.6	56.7	56.5	56.7	56.7	56.6	56.6	56.6	56.7
Total Electrical Input (kJ)	1340788	1440716	1299679	1524688	1401967	1335991	893502	1171015	1198900	1280917	1544164	1470126	15902453
Solar Fraction	59.31%	61.25%	52.83%	57.13%	37.04%	41.90%	30.66%	42.08%	52.96%	53.70%	47.02%	58.81%	50.22%
Preheat Tank Delta Energy (kJ)	4987	-1150	3769	-16191	12195	-7697	-1230	12798	-2847	-15599	17888	-3860	1810
Auxiliary Tank Delta Energy (kJ)	670	36	620	-242	-897	-192	655	-107	157	-178	506	-470	-171
Preheat Tank Data Gap Energy (kJ)	6707	626	-15725	0	-4862	-9804	-1366	-10760	-45170	-4395	0	0	-84748
Auxiliary Tank Data Gap Energy (kJ)	-463	7	727	0	1474	3234	-306	2571	-826	328	0	0	6745
Preheat Tank Energy Unbalance (kJ)	-11004	-12760	-15668	-12393	-18375	925	7990	14147	31718	34379	-9291	-7553	3366
Auxiliary Tank Energy Unbalance (kJ)	1822	20	3766	6993	12735	6927	5375	7073	2623	6017	3189	-1311	55956
Overall Energy Unbalance (kJ)	-9183	-12740	-11903	-5400	-5640	7852	13365	21220	34341	40396	-6101	-8864	59322

5.6.2 Experimental Measurement Uncertainty{ TC "5.6.2 Experimental Measurement Uncertainty" \l 3 }

The uncertainties associated with the experimental measurements as they appear in the monthly format of Table 5.6.1-1 were assessed. Estimates of the single sample uncertainties in the individual temperature, electrical power, and water draw measurements appear in Table 5.6.2-1. These uncertainties were propagated by standard techniques (Taylor, 1982) to arrive at probable uncertainties in tank electrical energy input, tank water heating load, tank heat loss, and average tank water temperature. Table 5.6.2-1 shows the resulting uncertainties in these results. A detailed formulation of the uncertainty propagation can be found in Appendix C.

Table 5.6.2-1 Estimated individual measurement uncertainties and resulting uncertainties in important system performance quantities.**{** TC **"Table 5.6.2-1** Estimated individual measurement uncertainties and resulting uncertainties in important system performance quantities.**" \l 6 }**

Quantity	Measurement Uncertainty	Uncertainty in Total/Average
average tank temperature	±1 C in individual Type T thermocouple measurement	± 1 C
tank heat loss	±1 C in individual Type T thermocouple measurement, ±5% in individual overall tank heat loss coefficient	± 6.4%
tank load	±0.3 C in individual Type T thermocouple measurement, ±1% in hourly water draw mass	± 2.3%
electrical energy input to preheat tank	±1% in voltage, ±1% in current	± 1.4%
electrical energy input to auxiliary tank	±1% in power	± 1.0%

5.6.3 TRNSYS Predicted Performance{ TC "5.6.3 TRNSYS Predicted Performance" \l 3 }

Table 5.6.3-1 shows the results of the TRNSYS simulation of the NIST prototype. The row labels in this table denote the same information as in Table 5.6.1-1 for the experimental data.

Table 5.6.3-2 presents the absolute discrepancy between the simulated and measured result tables. Finally, Table 5.6.3-3 shows the percentage discrepancy between the TRNSYS predictions and measurements for selected quantities in the previous tables. The tank energy unbalances noted in the TRNSYS simulation results in Table 5.6.3-1 resulted from a necessarily imperfect estimate of the true average temperature of each tank volume segment during a timestep. The model takes the arithmetic average of the initial and final segment temperatures in computing time-averaged energy flows. The resulting energy balance errors cannot be avoided but the effect on simulation accuracy is small (Newton, 1995).

Table 5.6.3-1 TRNSYS predicted performance results for the NIST system for July 1, 1995 through June 30, 1996.**{** TC **"Table 5.6.3-1** TRNSYS predicted performance results for the NIST system for July 1, 1995 through June 30, 1996." **\l 6 }**

Month	Jul	Aug	Sep	Oct	Nov	Dec	Jan	Feb	Mar	Apr	May	Jun	Total
Preheat Tank Load (kJ)	720888	786294	600203	763196	460183	512740	256525	453745	571351	639054	653745	796752	7214675
Auxiliary Tank Load (kJ)	503380	536635	585283	649479	833500	719974	578972	604927	473797	528788	770851	570967	7356552
Total Load (kJ)	1222156	1320656	1183950	1410610	1293016	1231712	835265	1057737	1043569	1166031	1423123	1365435	14553258
Preheat Tank Heat Loss (kJ)	18628	18152	7645	12887	-11796	-4172	-12390	-3088	10429	12495	767	18381	67940
Auxiliary Tank Heat Loss (kJ)	86994	93051	82008	98274	85722	81698	54998	71234	72632	82367	96330	96187	1001495
Water Draw (kg)	6492	6971	6253	7462	6741	6400	4330	5537	5541	6265	7469	7229	76691
Preheat Tank Electrical Input (kJ)	733927	800091	621991	760549	461029	509509	245012	474227	624222	642742	673559	807671	7354530
Auxiliary Tank Electrical Input (kJ)	589743	628292	664380	746300	918150	796114	633453	674207	542071	609453	869924	664977	8337064
Preheat Tank Average Temp. (C)	28.3	27.9	25.9	26.6	21.5	22.7	19.6	23.2	26.7	26.9	24.3	27.8	25.3
Auxiliary Tank Average Temp. (C)	55.5	55.5	55.1	55.3	54.5	54.8	54.3	54.7	55.1	55.2	54.9	55.5	55.1
Total Electrical Input (kJ)	1323670	1428383	1286371	1506849	1379179	1305623	878466	1148434	1166293	1252195	1543484	1472648	15691594
Solar Fraction	58.98%	59.54%	50.69%	54.10%	35.59%	41.63%	30.71%	42.90%	54.75%	54.81%	45.94%	58.35%	49.57%
Preheat Tank Delta Energy (kJ)	2997	-873	2315	-15273	11361	-6119	-2125	13103	-2192	-15420	17733	-5548	213
Auxiliary Tank Delta Energy (kJ)	-49	147	124	-1296	862	-163	-397	697	466	-916	1380	-195	-402
Preheat Tank Data Gap Energy (kJ)	8578	2852	-13030	0	-1314	-6597	-1144	-9460	-43476	-5433	0	0	-69024
Auxiliary Tank Data Gap Energy (kJ)	204	821	2447	0	1409	5524	1134	3272	5036	1245	0	0	21092
Preheat Tank Energy Unbalance (kJ)	-7	-630	-1202	-261	-33	463	1858	1007	1158	1181	1313	-1914	2679
Auxiliary Tank Energy Unbalance (kJ)	-378	-720	-588	-157	-525	128	1014	622	212	459	1363	-1982	509
Overall Energy Unbalance (kJ)	-385	-1350	-1790	-418	-558	591	2873	1629	1370	1640	2676	-3896	3188

Table 5.6.3-2 Absolute discrepancy between TRNSYS prediction and NIST measurement for July 1, 1995 through June 30, 1996.{ TC "**Table 5.6.3-2** Absolute discrepancy between TRNSYS prediction and NIST measurement for July 1, 1995 through June 30, 1996." \l 6 }

Month	Jul	Aug	Sep	Oct	Nov	Dec	Jan	Feb	Mar	Apr	May	Jun	Total
Preheat Tank Load (kJ)	-529	-15926	-18615	-34005	-16376	-5274	2384	10677	23035	20831	-8112	6000	-35911
Auxiliary Tank Load (kJ)	-4707	13021	16920	31440	7521	2272	7508	-153	-9137	-3686	11271	3535	75804
Total Load (kJ)	5766	10918	12634	15148	6257	-4664	6401	4901	8170	14861	15538	20743	116671
Preheat Tank Heat Loss (kJ)	-9020	-11483	-8406	-12130	-6285	-7722	-4070	-4762	-415	-87	-3900	-4246	-72526
Auxiliary Tank Heat Loss (kJ)	-6411	-6684	-6955	-7990	-10172	-8495	-6756	-7859	-6527	-6585	-9438	-6323	-90193
Water Draw (kg)	0	0	0	0	0	0	0	0	0	0	0	0	0
Preheat Tank Electrical Input (kJ)	-2414	-17228	-16704	-33086	-8701	-15086	-8936	-8221	-8978	-11238	-1562	5705	-126446
Auxiliary Tank Electrical Input (kJ)	-14704	4894	3395	15247	-14087	-15283	-6101	-14360	-23628	-17484	882	-3183	-84412
Preheat Tank Average Temp. (C)	-1.8	-2.2	-1.7	-2.2	-1.2	-1.6	-1.3	-1.1	0.1	0.1	-0.6	-0.6	-1.2
Auxiliary Tank Average Temp. (C)	-1.4	-1.3	-1.5	-1.4	-2.1	-1.9	-2.2	-2.0	-1.6	-1.4	-1.7	-1.1	-1.6
Total Electrical Input (kJ)	-17118	-12333	-13308	-17839	-22788	-30368	-15037	-22581	-32606	-28722	-681	2522	-210859
Solar Fraction	-0.32%	-1.71%	-2.14%	-3.02%	-1.45%	-0.27%	0.05%	0.81%	1.79%	1.10%	-1.08%	-0.45%	-0.65%
Preheat Tank Delta Energy (kJ)	-1990	277	-1454	918	-834	1579	-896	305	655	179	-155	-1688	-1597
Auxiliary Tank Delta Energy (kJ)	-719	111	-496	-1054	1759	29	-1053	804	309	-738	875	276	-231
Preheat Tank Data Gap Energy (kJ)	1872	2226	2694	0	3548	3207	222	1300	1694	-1037	0	0	15725
Auxiliary Tank Data Gap Energy (kJ)	667	814	1720	0	-65	2290	1440	700	5862	917	0	0	14346
Preheat Tank Energy Unbalance (kJ)	10997	12131	14466	12132	18342	-462	-6132	-13140	-30560	-33198	10604	5639	-688
Auxiliary Tank Energy Unbalance (kJ)	-2200	-740	-4353	-7150	-13260	-6799	-4360	-6452	-2411	-5558	-1827	-671	-55447
Overall Energy Unbalance (kJ)	8797	11391	10113	4982	5082	-7261	-10492	-19591	-32971	-38756	8777	4968	-56134

Table 5.6.3-3 Percentage discrepancy between TRNSYS prediction and NIST measurement for July 1, 1995 through June 30, 1996.{ TC "**Table 5.6.3-3** Percentage discrepancy between TRNSYS prediction and NIST measurement for July 1, 1995 through June 30, 1996." \l 6 }

Month	Jul	Aug	Sep	Oct	Nov	Dec	Jan	Feb	Mar	Apr	May	Jun	Total
Preheat Tank Load	-0.1%	-2.0%	-3.0%	-4.3%	-3.4%	-1.0%	0.9%	2.4%	4.2%	3.4%	-1.2%	0.8%	-0.5%
Auxiliary Tank Load	-0.9%	2.5%	3.0%	5.1%	0.9%	0.3%	1.3%	0.0%	-1.9%	-0.7%	1.5%	0.6%	1.0%
Total Load	0.5%	0.8%	1.1%	1.1%	0.5%	-0.4%	0.8%	0.5%	0.8%	1.3%	1.1%	1.5%	0.8%
Preheat Tank Heat Loss	-32.6%	-38.7%	-52.4%	-48.5%	-114.1%	-217.5%	-48.9%	-284.5%	-3.8%	-0.7%	-83.6%	-18.8%	-51.6%
Auxiliary Tank Heat Loss	-6.9%	-6.7%	-7.8%	-7.5%	-10.6%	-9.4%	-10.9%	-9.9%	-8.2%	-7.4%	-8.9%	-6.2%	-8.3%
Water Draw	0.0%	0.0%	0.0%	0.0%	0.0%	0.0%	0.0%	0.0%	0.0%	0.0%	0.0%	0.0%	0.0%
Preheat Tank Electrical Input	-0.3%	-2.1%	-2.6%	-4.2%	-1.9%	-2.9%	-3.5%	-1.7%	-1.4%	-1.7%	-0.2%	0.7%	-1.7%
Auxiliary Tank Electrical Input	-2.4%	0.8%	0.5%	2.1%	-1.5%	-1.9%	-1.0%	-2.1%	-4.2%	-2.8%	0.1%	-0.5%	-1.0%
Total Electrical Input	-1.3%	-0.9%	-1.0%	-1.2%	-1.6%	-2.3%	-1.7%	-1.9%	-2.7%	-2.2%	0.0%	0.2%	-1.3%

5.6.4 Comparison of Prediction and Experimental Data{ TC "5.6.4

Comparison of Prediction and Experimental Data" \l 3 }

5.6.4.1 The Overall System{ TC "5.6.4.1 The Overall System" \l 4 }

A comparison of the TRNSYS model performance in relation to the measured data is best accomplished by examining the results of the individual system components: the PV array and resistance controller, the preheat tank, and the auxiliary tank. Such analyses are presented in the following sections.

The TRNSYS simulation of the NIST system predicted the preheat tank, auxiliary tank, and overall system loads to within 0.5%, 1.0% and 0.8% of their measured values for the twelve month simulation, respectively. The simulation predicted the total preheat tank, auxiliary tank, and system electrical energy inputs to within 1.7%, 1.0%, and 1.3% of measured values, respectively. With the exception of the preheat tank electrical input, each of these discrepancies in the simulated results is less than the corresponding uncertainty in the simulated results. The twelve-month solar fraction measured by NIST was 50.2% while the simulation resulted in a solar fraction of 49.6%.

5.6.4.2 The PV Array Energy Output{ TC "5.6.4.2 The PV Array Energy Output" \l 4 }

The results in Table 5.6.3-3 show that the TRNSYS model of the NIST PV array predicted its electrical energy output to be 1.7% lower than was measured for twelve months of operation and to within 5.0% for each month of the period. The uncertainty in the measured result was ±1.4%. Close examination of the hourly simulation results indicated that the discrepancy followed a regular diurnal pattern. Figure 5.6.4.2-1 shows the average PV array energy output and the average *discrepancy* in PV energy output between prediction and measurement as a function of the hour of the day. The average hourly discrepancy is plotted both for a simulation in which the TRNSYS model calculated the PV array temperature independently and for one in which the array was assumed to be at exactly the measured temperature at all times. This figure indicates that the

model typically overpredicted energy output during early morning and late evening hours and tended to underpredict energy output during midday hours. This underprediction during midday hours was the dominant feature and led to an overall predicted result lower than measured.

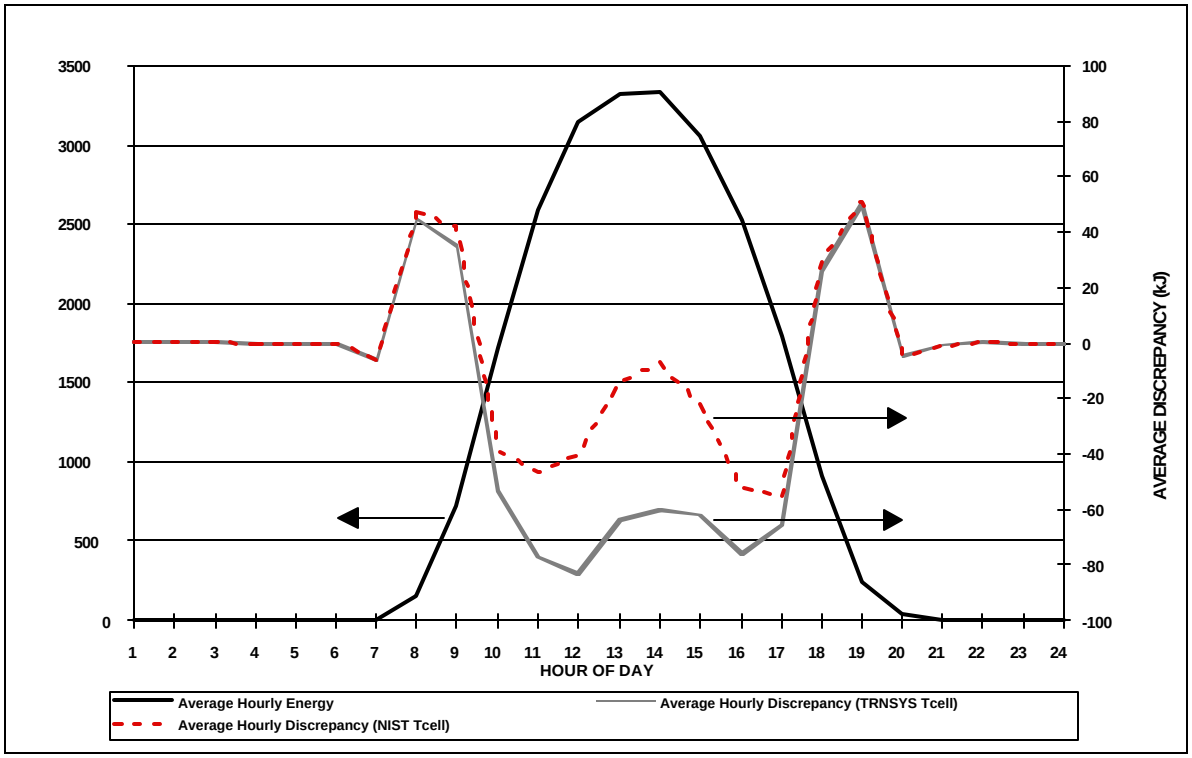

Figure 5.6.4.2-1 Average hourly PV array energy output and discrepancy between measurement and simulation as a function of the hour of day. Simulation results for the use of a TRNSYS-calculated array temperature and the NIST-measured temperature are shown.**{** TC **"Figure 5.6.4.2-1** Average hourly PV array energy output and discrepancy between measurement and simulation as a function of the hour of day. Simulation results for the use of a TRNSYS-calculated array temperature and the NIST-measured temperature are shown.**" \l 5 }**

A complete explanation for the pattern of discrepancy noted between the TRNSYS PV array model and the measured performance of the array at NIST proved elusive. The effect of irradiation incidence angle was considered as was the influence of the array temperature on power output. The array model made use of a very simple means of calculating array temperature which

may not have been satisfactory. Finally, other possibilities were identified but not studied in depth.

A pyranometer measures the total radiation on a surface, regardless of the incidence angle. As the incidence angle of radiation on the glass cover of a PV array is increased, it might be expected that a greater fraction of that radiation would be reflected or absorbed and not transmitted to the silicon PV cells. The TRNSYS model, which relied on pyranometer-measured irradiation to calculate the power output at any time, might then have overpredicted the power during morning and evening hours when the incidence angle of beam radiation was highest. Indeed, such a phenomenon appeared in the model results depicted in Figure 5.6.4.2-1. The data compiled by NIST in evaluating the reference module parameters lent additional credence to an incidence angle explanation for the morning and evening discrepancies. These data included array temperature, open circuit voltage, short circuit current, and voltage and current pairs at five or six different load resistances for over 200 combinations of ambient temperature, irradiance, and angle of incidence (Dougherty, 1996). The array used in these tests consisted of four parallel strings of ten series-wired Siemens M55 modules. Figures 5.6.4.2-2 and 5.6.4.2-3 present the percentage difference between the measured and predicted power as a function of irradiance and angle of incidence, respectively. Based on these figures, the discrepancy remained around zero except at irradiance levels lower than about 400 W/m^2 and angles of incidence greater than about 65 . Beyond these limits the model overpredicted array power quite dramatically. Irradiation angle of incidence, then, provides a reasonable explanation for the morning and evening discrepancies noted in Figure 5.6.4.2-1.

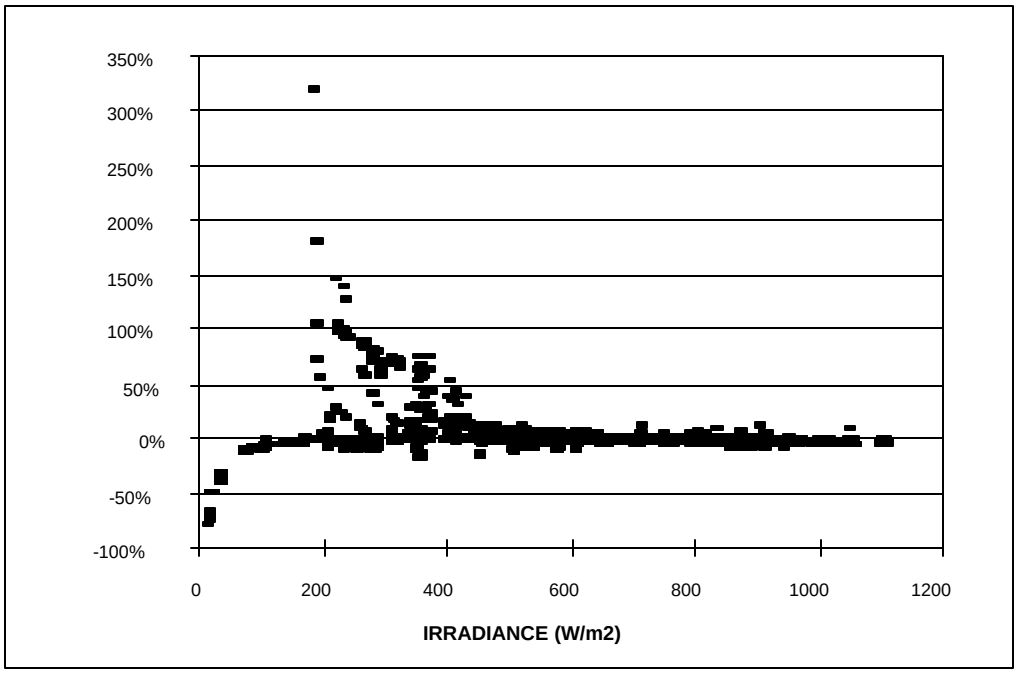

Figure 5.6.4.2-2 Percentage discrepancy in array power between TRNSYS model and measurements as a function of instantaneous irradiance level. Data from NIST module parameter determination.**{** TC **"Figure 5.6.4.2-2** Percentage discrepancy in array power between TRNSYS model and measurements as a function of instantaneous irradiance level. Data from NIST module parameter determination.**" \l 5 }**

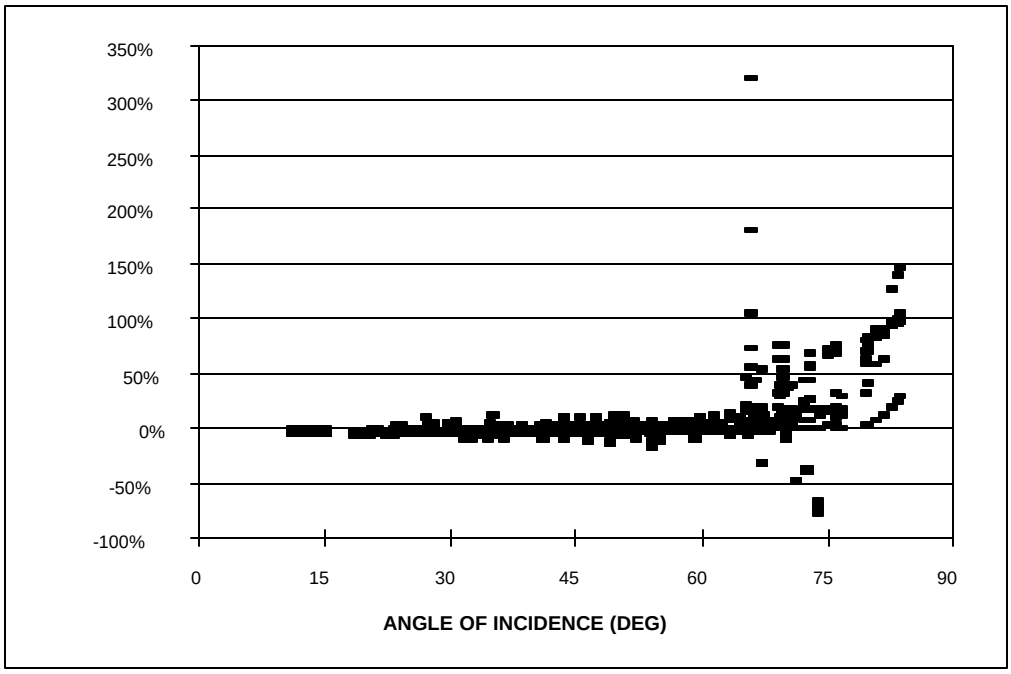

Figure 5.6.4.2-3 Percentage discrepancy in array power between TRNSYS model and measurements as a function of angle of incidence of irradiation. Data from NIST module parameter determination.**{** TC **"Figure 5.6.4.2-3** Percentage discrepancy in array power between TRNSYS model and measurements as a function of angle of incidence of irradiation. Data from NIST module parameter determination.**" \l 5 }**

The effect of the TRNSYS calculation of array temperature was also investigated. For the twelve month simulation, the TRNSYS array model resulted in an overall average array temperature of 19.3 C while the corresponding measured quantity was 18.1 C. When the model was run using the measured array temperature at each hour rather than an independently calculated one, the predicted total PV energy output rose by 1.2% and the overall discrepancy in this quantity fell to -0.5%. Figure 5.6.4.2-1 shows the impact of array temperature on the diurnal discrepancy pattern. It appears that the discrepancy was reduced to nearly zero around the noon hour as a result of correcting the array temperature. The error introduced to the model by the use of a simple array temperature calculation, then, provides a reasonable explanation for the discrepancy noted in Figure 5.6.4.2-1 around the noon hour.

As for the discrepancies not accounted for by incidence angle or array temperature effects,

these were likely the result of several factors. First, the PV array model itself was not a perfect representation of reality. The model used module performance results extracted from a single environmental condition and extrapolated these results to all other conditions based on some assumptions about the physics of a photovoltaic cell. The work of Townsend (1989) concluded that the model used by TRNSYS was accurate to about 5% around the maximum power point based on comparison with measured results from several module manufacturers. This 5% uncertainty was confirmed here in modeling the NIST prototype. Second, variations in the spectral composition of the radiation impinging on the array during a day or year may have impacted the resulting performance positively or negatively. The TRNSYS array model made no account for such effects and indeed, from a practical standpoint, experimental data on the spectral composition of solar radiation were not available. The PV module performance data chosen to form the reference parameters might have resulted from an environmental condition slightly out of the ordinary in atmospheric clarity, radiation spectral composition, or some other factor. This would have resulted in actual performance different from that suggested by this single test. The use of the measured total hourly irradiation (rather than minutely data) by the resistor-switching controller, resulting in resistive load changes only once each hour, may have affected the long-term prediction of PV energy output by about 0.5% as noted in Section 5.4. Finally, the use of pyranometer-measured irradiance data by the simulated controller instead of that of the reference PV cell (unavailable for the NIST system) may have affected the results from the TRNSYS PV array model.

5.6.4.3 The Preheat Tank Load and Heat Loss{ TC "5.6.4.3 The Preheat Tank Load and Heat Loss" \l 4 }

In order to examine the performance of the preheat tank model independent of any discrepancy in electrical input, the TRNSYS simulation of the NIST system was executed using the measured PV electrical energy output as the electrical input to the tank at each hour. It was

necessary to assume that this electrical energy was evenly distributed between the upper and lower resistive element clusters as the measured data indicated only the total electrical energy quantity. The results of this simulation are presented in Tables 5.6.4.3-1 through 5.6.4.3-3. The formats of these tables match those of Tables 5.6.3-1 through 5.6.3-3 presented above.

Table 5.6.4.3-1 TRNSYS predicted performance results for the NIST system for July 1, 1995 through June 30, 1996 (used electrical input to preheat tank and inlet water temperature to auxiliary tank measured by NIST).**{** TC **"Table 5.6.4.3-1** TRNSYS predicted performance results for the NIST system for July 1, 1995 through June 30, 1996 (used electrical input to preheat tank and inlet water temperature to auxiliary tank measured by NIST)." **\l 6 }**

Month	Jul	Aug	Sep	Oct	Nov	Dec	Jan	Feb	Mar	Apr	May	Jun	Total
Preheat Tank Load (kJ)	731896	807049	621595	794840	473417	528478	266587	466092	585617	653614	662199	794028	7385412
Auxiliary Tank Load (kJ)	514559	535253	581211	633573	832846	720802	578283	610695	496184	549109	775811	589084	7417410
Total Load (kJ)	1222353	1320800	1183600	1410223	1293099	1231927	835327	1057769	1048139	1167161	1422976	1365551	14558926
Preheat Tank Heat Loss (kJ)	14653	15302	6430	11353	-12470	-5023	-12241	-3991	8990	10924	-1400	13148	45674
Auxiliary Tank Heat Loss (kJ)	86794	92892	81822	98090	85524	81651	54945	71039	72442	82012	96126	95860	999195
Water Draw (kg)	6492	6971	6253	7462	6741	6400	4330	5537	5541	6265	7469	7229	76691
Preheat Tank Electrical Input (kJ)	736341	817319	638694	793635	469730	524595	253948	482448	633201	653980	675121	801966	7480977
Auxiliary Tank Electrical Input (kJ)	600826	626547	659939	730113	917304	796758	632614	679757	564793	628868	875034	682610	8395162
Preheat Tank Average Temp. (C)	27.2	27.1	25.5	26.2	21.3	22.4	19.6	22.9	26.3	26.5	23.8	26.6	24.8
Auxiliary Tank Average Temp. (C)	55.5	55.4	55.1	55.2	54.5	54.8	54.3	54.7	55.0	55.1	54.8	55.4	55.0
Total Electrical Input (kJ)	1337167	1443865	1298633	1523748	1387034	1321353	886562	1162204	1197994	1282848	1550155	1484575	15876139
Solar Fraction	59.88%	61.10%	52.52%	56.36%	36.61%	42.90%	31.91%	44.06%	55.87%	56.00%	46.54%	58.15%	50.73%
Preheat Tank Delta Energy (kJ)	629	-94	206	-12301	9202	-6117	-2961	11977	-1473	-12680	12998	-3314	-758
Auxiliary Tank Delta Energy (kJ)	-9	-5	47	-1397	975	-217	-396	965	-4	-1009	1730	-340	-488
Preheat Tank Data Gap Energy (kJ)	10838	4305	-10104	0	371	-6774	596	-7331	-38867	-904	0	0	-47869
Auxiliary Tank Data Gap Energy (kJ)	121	877	2662	0	1521	5591	1374	3575	4084	1769	0	0	21572
Preheat Tank Energy Unbalance (kJ)	1	-633	358	-256	-47	482	3159	1039	1200	1218	1325	-1896	2779
Auxiliary Tank Energy Unbalance (kJ)	-397	-716	-479	-152	-520	114	1156	632	255	525	1367	-1994	618
Overall Energy Unbalance (kJ)	-396	-1349	-120	-409	-567	595	4314	1671	1455	1743	2692	-3891	3397

Table 5.6.4.3-2 Absolute discrepancy between TRNSYS prediction and NIST measurement for July 1, 1995 through June 30, 1996 (used electrical input to preheat tank and inlet water temperature to auxiliary tank measured by NIST).**{** TC **"Table 5.6.4.3-2** Absolute discrepancy between TRNSYS prediction and NIST measurement for July 1, 1995 through June 30, 1996 (used electrical input to preheat tank and inlet water temperature to auxiliary tank measured by NIST)." **\l 6 }**

Month	Jul	Aug	Sep	Oct	Nov	Dec	Jan	Feb	Mar	Apr	May	Jun	Total
Preheat Tank Load (kJ)	10479	4829	2777	-2361	-3142	10464	12446	23024	37301	35391	342	3276	134826
Auxiliary Tank Load (kJ)	6472	11639	12848	15534	6867	3100	6819	5615	13250	16635	16231	21652	136662
Total Load (kJ)	5963	11062	12284	14761	6340	-4449	6463	4933	12740	15991	15391	20859	122339
Preheat Tank Heat Loss (kJ)	-12995	-14334	-9622	-13665	-6960	-8573	-3922	-5665	-1854	-1658	-6067	-9479	-94791
Auxiliary Tank Heat Loss (kJ)	-6611	-6844	-7141	-8174	-10371	-8542	-6809	-8054	-6717	-6940	-9642	-6649	-92494
Water Draw (kg)	0	0	0	0	0	0	0	0	0	0	0	0	0
Preheat Tank Electrical Input (kJ)	0	0	0	0	0	0	0	0	0	0	0	0	0
Auxiliary Tank Electrical Input (kJ)	-3620	3149	-1045	-940	-14933	-14638	-6940	-8811	-906	1931	5991	14450	-26314
Preheat Tank Average Temp. (C)	-2.8	-2.9	-2.1	-2.6	-1.4	-1.9	-1.3	-1.4	-0.4	-0.3	-1.1	-1.8	-1.7
Auxiliary Tank Average Temp. (C)	-1.4	-1.3	-1.5	-1.5	-2.2	-1.9	-2.2	-2.1	-1.7	-1.5	-1.8	-1.2	-1.7
Total Electrical Input (kJ)	-3620	3149	-1045	-940	-14933	-14638	-6940	-8811	-906	1931	5991	14450	-26314
Solar Fraction	0.57%	-0.15%	-0.31%	-0.77%	-0.42%	1.00%	1.25%	1.98%	2.92%	2.30%	-0.48%	-0.66%	0.50%
Preheat Tank Delta Energy (kJ)	-4358	1056	-3562	3890	-2993	1581	-1731	-821	1374	2920	-4890	546	-2568
Auxiliary Tank Delta Energy (kJ)	-679	-41	-573	-1155	1873	-25	-1051	1072	-161	-831	1225	130	-317
Preheat Tank Data Gap Energy (kJ)	4132	3679	5620	0	5233	3030	1962	3429	6302	3492	0	0	36879
Auxiliary Tank Data Gap Energy (kJ)	584	870	1935	0	47	2357	1680	1003	4910	1441	0	0	14827
Preheat Tank Energy Unbalance (kJ)	11005	12127	16027	12136	18328	-443	-4831	-13108	-30518	-33161	10616	5657	-587
Auxiliary Tank Energy Unbalance (kJ)	-2219	-736	-4244	-7145	-13255	-6813	-4219	-6441	-2368	-5492	-1823	-683	-55338
Overall Energy Unbalance (kJ)	8787	11391	11782	4991	5073	-7256	-9050	-19549	-32886	-38653	8793	4974	-55925

Table 5.6.4.3-3 Percentage discrepancy between TRNSYS prediction and NIST measurement for July 1, 1995 through June 30, 1996 (used electrical input to preheat tank and inlet water temperature to auxiliary tank measured by NIST).**{** TC **"Table 5.6.4.3-3** Percentage discrepancy between TRNSYS prediction and NIST measurement for July 1, 1995 through June 30, 1996 (used electrical input to preheat tank and inlet water temperature to auxiliary tank measured by NIST)." **\l 6 }**

Month	Jul	Aug	Sep	Oct	Nov	Dec	Jan	Feb	Mar	Apr	May	Jun	Total
Preheat Tank Load	1.5%	0.6%	0.4%	-0.3%	-0.7%	2.0%	4.9%	5.2%	6.8%	5.7%	0.1%	0.4%	1.9%
Auxiliary Tank Load	1.3%	2.2%	2.3%	2.5%	0.8%	0.4%	1.2%	0.9%	2.7%	3.1%	2.1%	3.8%	1.9%
Total Load	0.5%	0.8%	1.0%	1.1%	0.5%	-0.4%	0.8%	0.5%	1.2%	1.4%	1.1%	1.6%	0.8%
Preheat Tank Heat Loss	-47.0%	-48.4%	-59.9%	-54.6%	-126.3%	-241.5%	-47.1%	-338.4%	-17.1%	-13.2%	-130.0%	-41.9%	-67.5%
Auxiliary Tank Heat Loss	-7.1%	-6.9%	-8.0%	-7.7%	-10.8%	-9.5%	-11.0%	-10.2%	-8.5%	-7.8%	-9.1%	-6.5%	-8.5%
Water Draw	0.0%	0.0%	0.0%	0.0%	0.0%	0.0%	0.0%	0.0%	0.0%	0.0%	0.0%	0.0%	0.0%
Preheat Tank Electrical Input	0.0%	0.0%	0.0%	0.0%	0.0%	0.0%	0.0%	0.0%	0.0%	0.0%	0.0%	0.0%	0.0%
Auxiliary Tank Electrical Input	-0.6%	0.5%	-0.2%	-0.1%	-1.6%	-1.8%	-1.1%	-1.3%	-0.2%	0.3%	0.7%	2.2%	-0.3%
Total Electrical Input	-0.3%	0.2%	-0.1%	-0.1%	-1.1%	-1.1%	-0.8%	-0.8%	-0.1%	0.2%	0.4%	1.0%	-0.2%

Shown in Figure 5.6.4.3-1 are the measured and predicted monthly preheat tank loads. Error bars on the measured data represent the estimated uncertainties in these values based on the discussion above. Two sets of predicted results are shown in Figure 5.6.4.3-1: one in which the model analyzed the PV-SDHW system as a whole and one in which the preheat tank was modeled with errors introduced by the PV array suppressed (PV array electrical output fixed by measurement).

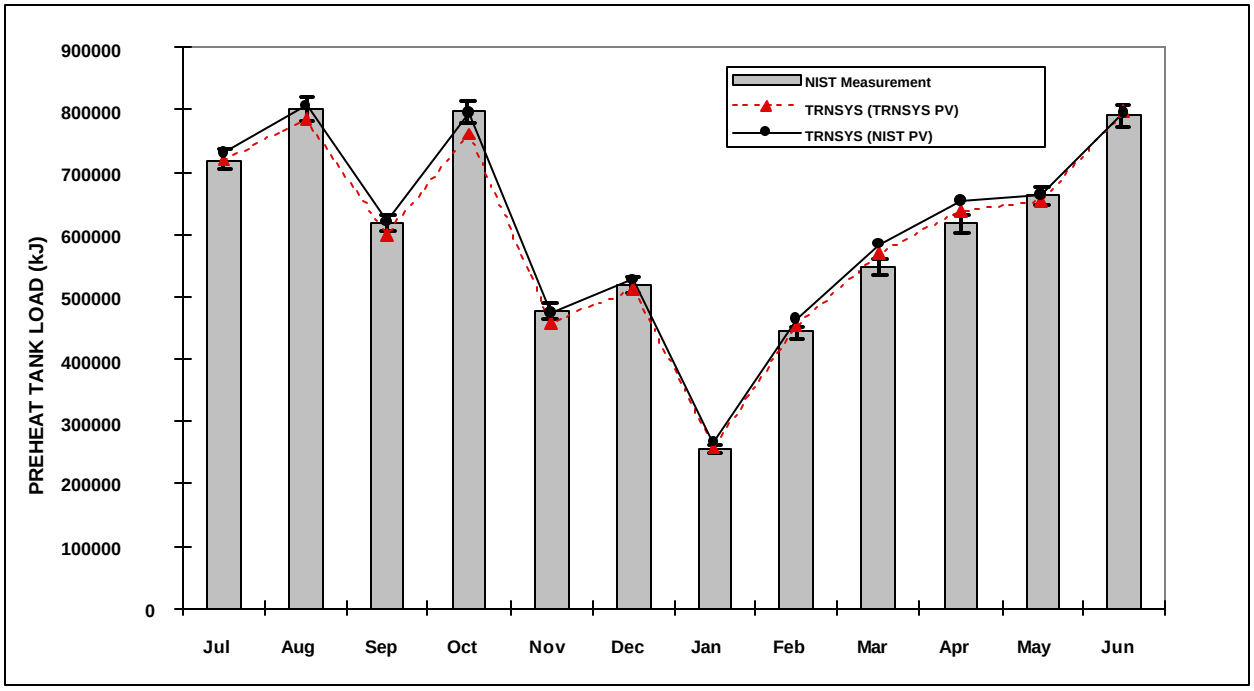

Figure 5.6.4.3-1 Measured and predicted monthly preheat tank water heating load. Predicted results with the electrical energy input determined by TRNSYS and measured by NIST are shown. Error bars on experimental data are 2.3%.**{** TC **"Figure 5.6.4.3-1** Measured and predicted monthly preheat tank water heating load. Predicted results with the electrical energy input determined by TRNSYS and measured by NIST are shown. Error bars on experimental data are 2.3%." **\l 5 }**

Table 5.6.4.3-3 indicates that, despite having exactly the measured electrical input, the

simulated preheat tank load for the NIST system was about 1.9% higher than measured for the twelve month analysis. This load prediction falls within the estimated ±2.3% uncertainty in the measured data.

The simulated preheat tank average temperature was 1.7 C lower than measured and the heat loss was 67.5% low (although this percentage is large, the tank heat loss was a small quantity - less than 2.0% of the energy added to the tank - so the absolute error is small). The corresponding measurement uncertainties were ±1.0 C and ±6.4%, respectively. In order to find the origin of the tank temperature discrepancy, minutely tank temperature distributions for May 15-23, 1996 were studied. These data indicated that the most significant discrepancy in tank node temperature occurred in the bottom node. During these nine days, the predicted average temperature for the top five nodes averaged 0.5 C lower than measured while that of the sixth node averaged 5.6 C lower. Noting that the monthly preheat tank energy unbalances in the simulated results were substantially smaller than those measured (0.2% versus 2.4% of the total energy added to the tank), the possibility must be considered that the measured bottom-node tank temperature did not accurately represent the average temperature of the bottom sixth of the tank. The placement of the thermocouple for this measurement too close to the lower resistor cluster, for example, might have resulted in an inaccurate representation of the *average* temperature in the region. Indeed, very sharp temperature inclines are possible in the bottom node, complicating the placement of a thermocouple to measure the average temperature. An overstatement of this temperature in the measured data would lead to an overstatement of the average tank temperature and subsequently to an overstatement of tank heat losses. The overstatement of measured temperature by 1.7 C throughout the simulation period approximately accounts for the noted discrepancy in preheat tank heat losses.

5.6.4.4 The Auxiliary Tank Load and Heat Loss{ TC "5.6.4.4 The Auxiliary Tank Load and Heat Loss" \l 4 }

In order to examine the performance of the auxiliary tank model independent of the effect of the inlet water temperature from the preheat tank, a simulation of the NIST PV-SDHW prototype was run with the inlet water temperature to this tank fixed by the measured temperature during draws. Tables 5.6.4.3-1 through 5.6.4.3-3 show the results of this simulation. Shown in Figure 5.6.4.4-1 are the measured and predicted monthly auxiliary tank loads. Error bars on the measured data represent the estimated uncertainties in these values based on the discussion above. Two sets of predicted results are shown in Figure 5.6.4.4-1: one in which the model analyzed the PV-SDHW system as a whole and one in which the auxiliary tank was modeled with errors introduced by the preheat tank suppressed (inlet water temperature fixed by measurement).

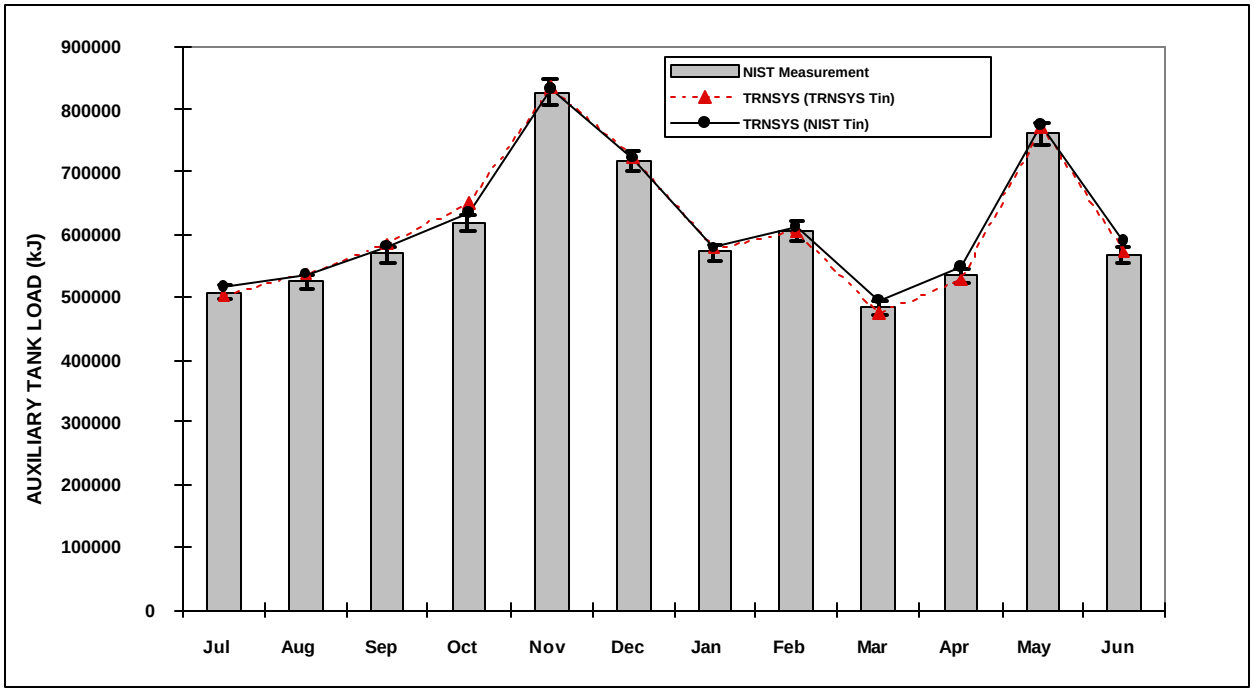

Figure 5.6.4.4-1 Measured and predicted monthly auxiliary tank water heating load. Predicted results with the inlet water temperature determined by TRNSYS and measured by NIST are shown. Error bars on experimental data are 2.3%.**{** TC **"Figure 5.6.4.4-1** Measured and predicted monthly auxiliary tank water heating load. Predicted results with the inlet water temperature determined by TRNSYS and measured by NIST are shown. Error bars on experimental data are 2.3%.**" \l 5 }**

Table 5.6.4.3-3 indicates that with the simulation inlet water temperature set to the measured value for each draw hour, the auxiliary tank model underpredicted the electrical energy consumption by just 0.3% when the thermostat setpoint was 58.6 C. However, the simulation overpredicted the tank load by 1.9%. The uncertainties in the measured electrical energy input and tank load were ±1.0% and ±2.3%, respectively. The auxiliary tank average temperature and heat loss determined by the simulation were 1.7 C and 8.5% lower, respectively, than the measured quantities, similar to the result for the preheat tank simulation. The measurement uncertainties in average temperature and heat loss were ±1.0 C and ±6.4%, respectively. For the minutely simulation of May 15-23, 1996, the average temperature predicted by the model for the top five nodes was just 0.4 C higher than measured while that for the sixth node was 13.5 C lower than measured. This evidence gives further credence to the suggestion that the placement of the thermocouple for the bottom tank node temperature resulted in measurements which did not represent the average temperature of that region. The monthly auxiliary tank energy unbalances in the simulated data were small compared with those implicit in the measured data (0.1% versus 0.7% of the total energy added to the tank).

5.7 Modeling the FSEC Prototype{ TC "5.7 Modeling the FSEC Prototype" \l 2 }

In order to further examine the adequacy of the TRNSYS model of a PV-SDHW system, the performance of the prototype installed at FSEC was simulated and the model output compared with measured results.

5.7.1 Experimental Measurements{ TC "5.7.1 Experimental Measurements" \l 3 }

Table 5.7.1-1 presents the experimental results measured from the prototype installed at FSEC for the period of December 23, 1995 through September 26, 1996. The format of this table

matches its counterpart in Table 5.6.1-1 for the NIST system.

Table 5.7.1-1 FSEC performance results for the period December 23, 1995 through September 26, 1996.**{** TC **"Table 5.7.1-1** FSEC performance results for the period December 23, 1995 through September 26, 1996." **\l 6 }**

Month	Dec	Jan	Feb	Mar	Apr	May	Jun	Jul	Aug	Sep	Total
Preheat Tank Load (kJ)	146949	552753	626603	680776	524391	670472	555283	555553	559099	468948	5340827
Auxiliary Tank Load (kJ)	164384	446806	276857	281551	119665	90405	157034	68248	99452	132578	1836981
Total Load (kJ)	309418	992167	895864	955211	639744	755481	707977	619581	653511	596996	7125949
Preheat Tank Heat Loss (kJ)	10834	51681	60326	68231	58668	87486	77083	79564	80616	66027	640517
Auxiliary Tank Heat Loss (kJ)	33204	110904	101156	108172	76207	97458	93860	84090	89255	79298	873603
Water Draw (kg)	2163	7462	6992	7487	5542	7497	7229	6537	7080	6328	64316
Preheat Tank Electrical Input (kJ)	155397	607320	666870	741240	573369	757329	628248	637255	618882	528387	5914296
Auxiliary Tank Electrical Input (kJ)	192971	544615	367054	379045	191505	177073	247242	140495	178757	208169	2626926
Preheat Tank Average Temp. (C)	27.0	30.3	33.4	34.1	37.2	39.3	37.8	40.2	39.2	38.0	36.2
Auxiliary Tank Average Temp. (C)	50.4	50.4	50.5	50.6	50.4	49.7	49.4	49.7	49.3	49.1	49.9
Total Electrical Input (kJ)	348368	1151935	1033924	1120286	764874	934402	875490	777749	797638	736555	8541222
Solar Fraction	47.49%	55.71%	69.94%	71.27%	81.97%	88.75%	78.43%	89.67%	85.55%	78.55%	74.95%
Preheat Tank Delta Energy (kJ)	442	14901	-9248	6776	-4875	7622	4851	720	-4375	1225	17462
Auxiliary Tank Delta Energy (kJ)	433	87	-630	-535	11	-2076	2320	1374	-3339	1239	-1411
Preheat Tank Data Gap Energy (kJ)	0	0	0	0	-1267	0	0	-7418	9329	0	644
Auxiliary Tank Data Gap Energy (kJ)	0	0	0	0	-3571	0	0	9126	5836	0	11390
Preheat Tank Energy Unbalance (kJ)	-2828	-12015	-10811	-14543	-6081	-8252	-8969	-6001	-7130	-7813	-83865
Auxiliary Tank Energy Unbalance (kJ)	-5050	-13182	-10328	-10143	-7950	-8713	-5972	-4092	-776	-4946	-70857
Overall Energy Unbalance (kJ)	-7878	-25197	-21138	-24686	-14031	-16965	-14941	-10092	-7905	-12759	-154721

5.7.2 Experimental Measurement Uncertainty{ TC "5.7.2 Experimental Measurement Uncertainty" \l 3 }

The FSEC prototype system was instrumented in identical fashion to that at NIST. Therefore, experimental measurement uncertainties and uncertainties in calculated system performance results were considered to be the same at FSEC as at NIST and appear in Table 5.6.2-1.

5.7.3 TRNSYS Predicted Performance{ TC "5.7.3 TRNSYS Predicted Performance" \l 3 }

Table 5.7.3-1 presents the results of the TRNSYS simulation of the FSEC system. Tables 5.7.3-2 and 5.7.3-3 show the absolute and percentage discrepancies, respectively, between the TRNSYS prediction and FSEC measurements. These tables are identical in structure to those presented in Tables 5.6.3-1 through 5.6.3-3 for the NIST prototype.

Table 5.7.3-1 TRNSYS predicted performance results for the FSEC system for December 23, 1995 through September 26, 1996.**{** TC **"Table 5.7.3-1** TRNSYS predicted performance results for the FSEC system for December 23, 1995 through September 26, 1996." **\l 6 }**

Month	Dec	Jan	Feb	Mar	Apr	May	Jun	Jul	Aug	Sep	Total
Preheat Tank Load (kJ)	151030	567331	648939	709402	557414	718086	594620	588309	598779	500447	5634358
Auxiliary Tank Load (kJ)	154740	413264	242890	244710	100610	58358	114337	58972	68919	95179	1551976
Total Load (kJ)	305172	978085	888871	950837	655279	772627	705649	643966	664306	592833	7157625
Preheat Tank Heat Loss (kJ)	10051	47799	57146	64783	57918	86680	76934	77993	80791	65598	625693
Auxiliary Tank Heat Loss (kJ)	31441	106007	97705	103789	71585	91516	88427	79267	84343	75243	829322
Water Draw (kg)	2163	7462	6992	7487	5542	7497	7229	6537	7080	6328	64316
Preheat Tank Electrical Input (kJ)	161693	629332	697080	781112	607818	813941	676298	675289	668058	568612	6279232
Auxiliary Tank Electrical Input (kJ)	184379	519393	340834	348494	173703	148596	203500	126331	147025	171004	2363258
Preheat Tank Average Temp. (C)	26.7	29.9	33.1	33.8	37.4	39.6	38.1	40.3	39.5	38.2	36.2
Auxiliary Tank Average Temp. (C)	48.3	48.6	48.8	48.7	48.0	47.4	47.1	47.4	47.1	47.1	47.8
Total Electrical Input (kJ)	346072	1148725	1037913	1129606	781521	962537	879798	801620	815082	739616	8642490
Solar Fraction	49.49%	58.00%	73.01%	74.61%	85.07%	92.94%	84.27%	91.36%	90.14%	84.42%	78.72%
Preheat Tank Delta Energy (kJ)	652	14139	-8523	7252	-5819	9404	4139	273	-3584	1689	18931
Auxiliary Tank Delta Energy (kJ)	-1641	412	440	209	-758	-1170	665	662	-793	519	-2590
Preheat Tank Data Gap Energy (kJ)	0	0	0	0	1341	0	0	-7768	8842	0	2415
Auxiliary Tank Data Gap Energy (kJ)	0	0	0	0	-2520	0	0	12377	5531	0	15388
Preheat Tank Energy Unbalance (kJ)	-40	62	-482	-325	-353	-229	605	946	913	878	2665
Auxiliary Tank Energy Unbalance (kJ)	-161	-290	-200	-214	-253	-108	72	-193	86	63	-62
Overall Energy Unbalance (kJ)	-202	-228	-683	-539	-606	-337	677	753	999	940	2603

Table 5.7.3-2 Absolute discrepancy between TRNSYS prediction and FSEC measurement for December 23, 1995 through September 26, 1996.**{** TC **"Table 5.7.3-2** Absolute discrepancy between TRNSYS prediction and FSEC measurement for December 23, 1995 through September 26, 1996." **\l 6 }**

Month	Dec	Jan	Feb	Mar	Apr	May	Jun	Jul	Aug	Sep	Total
Preheat Tank Load (kJ)	4081	14579	22336	28625	33023	47614	39337	32756	39681	31499	293531
Auxiliary Tank Load (kJ)	-9645	-33542	-33967	-36842	-19056	-32047	-42698	-9276	-30534	-37399	-285005
Total Load (kJ)	-4246	-14081	-6993	-4374	15534	17146	-2328	24385	10796	-4164	31675
Preheat Tank Heat Loss (kJ)	-784	-3882	-3180	-3448	-750	-806	-149	-1571	175	-428	-14823
Auxiliary Tank Heat Loss (kJ)	-1762	-4897	-3451	-4384	-4622	-5942	-5433	-4824	-4912	-4055	-44281
Water Draw (kg)	0	0	0	0	0	0	0	0	0	0	0
Preheat Tank Electrical Input (kJ)	6296	22011	30210	39872	34449	56612	48050	38034	49176	40225	364936
Auxiliary Tank Electrical Input (kJ)	-8592	-25222	-26221	-30552	-17802	-28478	-43742	-14164	-31732	-37165	-263668
Preheat Tank Average Temp. (C)	-0.3	-0.4	-0.3	-0.3	0.1	0.2	0.3	0.0	0.3	0.2	0.0
Auxiliary Tank Average Temp. (C)	-2.1	-1.8	-1.7	-1.9	-2.5	-2.4	-2.3	-2.3	-2.2	-2.0	-2.1
Total Electrical Input (kJ)	-2296	-3211	3989	9320	16647	28134	4308	23871	17444	3060	101268
Solar Fraction	2.00%	2.29%	3.06%	3.34%	3.10%	4.19%	5.83%	1.69%	4.58%	5.86%	3.77%
Preheat Tank Delta Energy (kJ)	211	-762	726	476	-943	1782	-712	-447	791	464	1470
Auxiliary Tank Delta Energy (kJ)	-2074	325	1070	745	-769	906	-1655	-712	2546	-719	-1179
Preheat Tank Data Gap Energy (kJ)	0	0	0	0	2608	0	0	-350	-487	0	1771
Auxiliary Tank Data Gap Energy (kJ)	0	0	0	0	1051	0	0	3251	-305	0	3998
Preheat Tank Energy Unbalance (kJ)	2787	12077	10328	14218	5728	8023	9574	6947	8042	8691	86530
Auxiliary Tank Energy Unbalance (kJ)	4889	12892	10128	9929	7697	8605	6043	3899	862	5009	70795
Overall Energy Unbalance (kJ)	7676	24969	20456	24147	13424	16628	15618	10846	8904	13700	157324

Table 5.7.3-3 Percentage discrepancy between TRNSYS prediction and FSEC measurement for December 23, 1995 through September 26, 1996.**{** TC **"Table 5.7.3-3** Percentage discrepancy between TRNSYS prediction and FSEC measurement for December 23, 1995 through September 26, 1996." **\l 6 }**

Month	Dec	Jan	Feb	Mar	Apr	May	Jun	Jul	Aug	Sep	Total
Preheat Tank Load	2.8%	2.6%	3.6%	4.2%	6.3%	7.1%	7.1%	5.9%	7.1%	6.7%	5.5%
Auxiliary Tank Load	-5.9%	-7.5%	-12.3%	-13.1%	-15.9%	-35.4%	-27.2%	-13.6%	-30.7%	-28.2%	-15.5%
Total Load	-1.4%	-1.4%	-0.8%	-0.5%	2.4%	2.3%	-0.3%	3.9%	1.7%	-0.7%	0.4%
Preheat Tank Heat Loss	-7.2%	-7.5%	-5.3%	-5.1%	-1.3%	-0.9%	-0.2%	-2.0%	0.2%	-0.6%	-2.3%
Auxiliary Tank Heat Loss	-5.3%	-4.4%	-3.4%	-4.1%	-6.1%	-6.1%	-5.8%	-5.7%	-5.5%	-5.1%	-5.1%
Water Draw	0.0%	0.0%	0.0%	0.0%	0.0%	0.0%	0.0%	0.0%	0.0%	0.0%	0.0%
Preheat Tank Electrical Input	4.1%	3.6%	4.5%	5.4%	6.0%	7.5%	7.6%	6.0%	7.9%	7.6%	6.2%
Auxiliary Tank Electrical Input	-4.5%	-4.6%	-7.1%	-8.1%	-9.3%	-16.1%	-17.7%	-10.1%	-17.8%	-17.9%	-10.0%
Total Electrical Input	-0.7%	-0.3%	0.4%	0.8%	2.2%	3.0%	0.5%	3.1%	2.2%	0.4%	1.2%

5.7.4 Comparison of Prediction and Experimental Data{ TC "5.7.4 Comparison of Prediction and Experimental Data" \l 3 }

5.7.4.1 The Overall System{ TC "5.7.4.1 The Overall System" \l 4 }

A comparison of simulation and measurement for the FSEC system was conducted in the same manner as for the NIST system discussed above. The examinations of the individual components will be presented in the sections that follow.

The TRNSYS simulation of the FSEC system predicted the preheat tank, auxiliary tank, and overall system loads to within 5.5%, 15.5%, and 0.4%, respectively for the nine month simulation. Measurement uncertainties in these quantities were ±2.3%. The preheat tank, auxiliary tank, and total electrical energy inputs were predicted to within 6.2%, 10.0%, and 1.2%, respectively. The corresponding measurement uncertainties were ±1.4%, ±1.0%, and about ±1.2%, respectively. The nine-month solar fraction measured by FSEC was 74.9% while the simulation resulted in a solar fraction of 78.7%. The differences between simulation and measurement were primarily the result of a large discrepancy in the performance of the PV array as discussed below.

5.7.4.2 The PV Array Energy Output{ TC "5.7.4.2 The PV Array Energy Output" \l 4 }

Table 5.7.3-3 shows that the TRNSYS model overpredicted the PV array energy output by 6.2% during the nine month simulation. This discrepancy exceeded the measurement uncertainty of ±1.4%. Figure 5.7.4.2-1 indicates that the discrepancy occurred consistently throughout the average day.

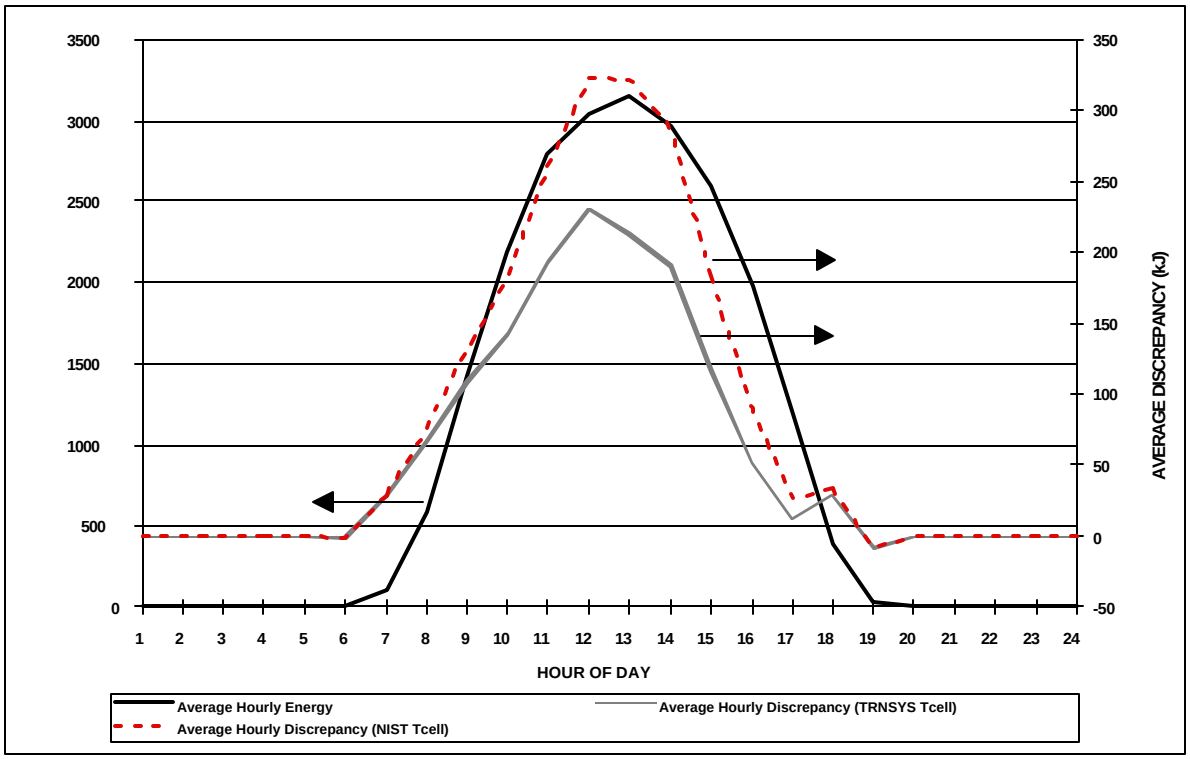

Figure 5.7.4.2-1 Average hourly PV array energy output and discrepancy between measurement and simulation as a function of the hour of day. Simulation results for the use of a TRNSYS-calculated array temperature and the FSEC-measured temperature are shown.**{** TC **"Figure 5.7.4.2-1** Average hourly PV array energy output and discrepancy between measurement and simulation as a function of the hour of day. Simulation results for the use of a TRNSYS-calculated array temperature and the FSEC-measured temperature are shown.**" \l 5 }**

The pattern of PV energy discrepancy noted in Figure 5.7.4.2-1 is remarkably different from that shown in Figure 5.6.4.2-1 for the NIST prototype. In this case, a consistent overprediction occurs both during morning and evening and during the middle of the day. While a consideration of incidence angle effects may help explain the discrepancies noted during morning and evening, the large discrepancy throughout the rest of the day suggests some systematic difference in the actual operating conditions and those assumed by the model. The factor of array temperature worked here in the opposite direction from correcting the discrepancy. TRNSYS predicted an overall average array temperature of 26.8 C using a simple balance of energy while

the average measured value was 24.5 C. As seen in Figure 5.7.4.2-1, using lower measured array temperature would in fact widen the discrepancy in array energy output. Thus the factors thought most important in the case of the NIST simulation discrepancy were little help in the case of the FSEC discrepancy.

The true cause of the large discrepancy in PV energy output for the FSEC system could not be determined. Possible contributors to this pattern, however, were identified. First, one or more of the PV modules used in the array at FSEC may have been defective, malfunctioning, or in some way not operating in line with the performance parameters measured for that type of module at NIST in the past. Since the PV modules used in the two installations were of the same make and model, it had to be assumed that the same model parameters must apply in both cases. Second, the model might have consistently overpredicted the power if the total irradiation contained a large fraction which was diffuse, as diffuse radiation is known to have a large effective angle of incidence - about 60 (Duffie and Beckman, 1991). While the annual average clearness index in Cocoa, FL is slightly higher than in Gaithersburg, MD (Duffie and Beckman, 1991), the climate in Cocoa is known for creating a high fraction of diffuse radiation due to suspended moisture in the atmosphere. Thus it is conceivable that if such bright, hazy conditions existed consistently during the operation of the FSEC prototype, the energy output of the PV array there would be less than that suggested by the measured total solar irradiation and ambient temperature. Third, the wiring of the array, switching controller, and resistors may have been connected in a manner different from that at NIST leading somehow to inferior performance. Ultimately, only two known differences existed between the two PV system installations: the number and arrangement of the modules in the array and the frequency of controller switching decisions. The first of these was correctly accounted for in the TRNSYS array models and the second was considered to be of negligible importance in light of the fact that the model made switching decisions only once each hour anyway.

5.7.4.3 The Preheat Tank Load and Heat Loss{ TC "5.7.4.3 The Preheat Tank

Load and Heat Loss" \l 4 **}**

Tables 5.7.4.3-1, 5.7.4.3-2, and 5.7.4.3-3 show the results of an independent examination of the TRNSYS preheat tank model in simulating the FSEC system. Figure 5.7.4.3-1 shows the measured and predicted monthly preheat tank loads. This figure shows results from a simulation using the TRNSYS-calculated PV energy output and that measured by FSEC.

Table 5.7.4.3-1 TRNSYS predicted performance results for the FSEC system for December 23, 1995 through September 26, 1996 (used electrical input to preheat tank and inlet water temperature to auxiliary tank measured by FSEC).**{** TC **"Table 5.7.4.3-1** TRNSYS predicted performance results for the FSEC system for December 23, 1995 through September 26, 1996 (used electrical input to preheat tank and inlet water temperature to auxiliary tank measured by FSEC)." **\l 6 }**

Month	Dec	Jan	Feb	Mar	Apr	May	Jun	Jul	Aug	Sep	Total
Preheat Tank Load (kJ)	145532	553019	623653	677062	529662	673228	553911	558558	559412	467549	5341587
Auxiliary Tank Load (kJ)	160614	435792	276134	287394	115289	84644	146455	76900	97398	127619	1808239
Total Load (kJ)	305449	980077	893548	959082	634051	748296	696258	627243	650929	591830	7086762
Preheat Tank Heat Loss (kJ)	8775	42503	50944	58070	52046	78048	69696	71353	73262	59476	564173
Auxiliary Tank Heat Loss (kJ)	31362	105780	97559	103932	71683	91268	88908	79610	85357	75607	831065
Water Draw (kg)	2163	7462	6992	7487	5542	7497	7229	6537	7080	6328	64316
Preheat Tank Electrical Input (kJ)	155397	607320	666870	741240	573369	757329	628248	637255	618882	528387	5914297
Auxiliary Tank Electrical Input (kJ)	190017	542395	373228	391638	188110	174225	236585	144901	177716	203898	2622713
Preheat Tank Average Temp. (C)	25.8	28.9	31.8	32.5	35.8	37.9	36.6	38.8	38.0	36.8	34.8
Auxiliary Tank Average Temp. (C)	48.3	48.5	48.8	48.8	48.0	47.4	47.3	47.6	47.4	47.3	47.9
Total Electrical Input (kJ)	345414	1149715	1040097	1132879	761479	931554	864833	782156	796598	732285	8537010
Solar Fraction	47.65%	56.43%	69.80%	70.59%	83.54%	89.97%	79.56%	89.05%	85.94%	79.00%	75.37%
Preheat Tank Delta Energy (kJ)	1128	11733	-7272	6418	-3959	6275	4067	1401	-4166	532	15550
Auxiliary Tank Delta Energy (kJ)	-1793	1087	-243	492	-1073	-1575	-1248	996	-1612	-438	-3204
Preheat Tank Data Gap Energy (kJ)	0	0	0	0	4042	0	0	-5035	10474	0	9481
Auxiliary Tank Data Gap Energy (kJ)	0	0	0	0	-2461	0	0	12460	6552	0	16551
Preheat Tank Energy Unbalance (kJ)	-39	66	-455	-310	-338	-223	574	908	849	829	2468
Auxiliary Tank Energy Unbalance (kJ)	-165	-264	-223	-180	-250	-113	2470	-145	3125	1110	3163
Overall Energy Unbalance (kJ)	-204	-198	-678	-489	-588	-335	3044	763	3973	1939	5631

Table 5.7.4.3-2 Absolute discrepancy between TRNSYS prediction and FSEC measurement for December 23, 1995 through September 26, 1996 (used electrical input to preheat tank and inlet water temperature to auxiliary tank measured by FSEC).**{** TC **"Table 5.7.4.3-2** Absolute discrepancy between TRNSYS prediction and FSEC measurement for December 23, 1995 through September 26, 1996 (used electrical input to preheat tank and inlet water temperature to

auxiliary tank measured by FSEC)." \l 6 }

Month	Dec	Jan	Feb	Mar	Apr	May	Jun	Jul	Aug	Sep	Total
Preheat Tank Load (kJ)	-1417	266	-2949	-3714	5272	2756	-1372	3005	313	-1399	760
Auxiliary Tank Load (kJ)	-3770	-11015	-723	5843	-4376	-5761	-10580	8652	-2054	-4959	-28743
Total Load (kJ)	-3969	-12090	-2316	3871	-5694	-7185	-11719	7663	-2582	-5166	-39187
Preheat Tank Heat Loss (kJ)	-2059	-9178	-9382	-10161	-6622	-9438	-7387	-8211	-7354	-6550	-76343
Auxiliary Tank Heat Loss (kJ)	-1842	-5124	-3597	-4240	-4523	-6190	-4951	-4480	-3898	-3691	-42537
Water Draw (kg)	0	0	0	0	0	0	0	0	0	0	0
Preheat Tank Electrical Input (kJ)	0	0	0	0	0	0	0	0	0	0	1
Auxiliary Tank Electrical Input (kJ)	-2954	-2220	6173	12593	-3395	-2848	-10657	4407	-1041	-4271	-4213
Preheat Tank Average Temp. (C)	-1.1	-1.5	-1.6	-1.6	-1.4	-1.4	-1.2	-1.4	-1.2	-1.2	-1.4
Auxiliary Tank Average Temp. (C)	-2.1	-1.9	-1.7	-1.8	-2.4	-2.4	-2.1	-2.2	-1.9	-1.9	-2.0
Total Electrical Input (kJ)	-2954	-2220	6174	12593	-3395	-2848	-10657	4407	-1041	-4270	-4212
Solar Fraction	0.15%	0.71%	-0.15%	-0.67%	1.57%	1.22%	1.12%	-0.62%	0.39%	0.45%	0.43%
Preheat Tank Delta Energy (kJ)	687	-3168	1976	-358	917	-1347	-784	681	208	-693	-1911
Auxiliary Tank Delta Energy (kJ)	-2226	1000	388	1028	-1085	502	-3568	-378	1728	-1677	-1792
Preheat Tank Data Gap Energy (kJ)	0	0	0	0	5309	0	0	2383	1145	0	8837
Auxiliary Tank Data Gap Energy (kJ)	0	0	0	0	1110	0	0	3334	716	0	5161
Preheat Tank Energy Unbalance (kJ)	2789	12080	10355	14233	5743	8029	9543	6908	7978	8642	86332
Auxiliary Tank Energy Unbalance (kJ)	4885	12918	10105	9963	7700	8601	8442	3947	3900	6056	74020
Overall Energy Unbalance (kJ)	7674	24999	20460	24196	13443	16630	17985	10855	11879	14698	160353

Table 5.7.4.3-3 Percentage discrepancy between TRNSYS prediction and FSEC measurement for December 23, 1995 through September 26, 1996 (used electrical input to preheat tank and inlet water temperature to auxiliary tank measured by FSEC).**{** TC **"Table 5.7.4.3-3** Percentage discrepancy between TRNSYS prediction and FSEC measurement for December 23, 1995 through September 26, 1996 (used electrical input to preheat tank and inlet water temperature to auxiliary tank measured by FSEC)." \l 6 }

Month	Dec	Jan	Feb	Mar	Apr	May	Jun	Jul	Aug	Sep	Total
Preheat Tank Load	-1.0%	0.0%	-0.5%	-0.5%	1.0%	0.4%	-0.2%	0.5%	0.1%	-0.3%	0.0%
Auxiliary Tank Load	-2.3%	-2.5%	-0.3%	2.1%	-3.7%	-6.4%	-6.7%	12.7%	-2.1%	-3.7%	-1.6%
Total Load	-1.3%	-1.2%	-0.3%	0.4%	-0.9%	-1.0%	-1.7%	1.2%	-0.4%	-0.9%	-0.5%
Preheat Tank Heat Loss	-19.0%	-17.8%	-15.6%	-14.9%	-11.3%	-10.8%	-9.6%	-10.3%	-9.1%	-9.9%	-11.9%
Auxiliary Tank Heat Loss	-5.5%	-4.6%	-3.6%	-3.9%	-5.9%	-6.4%	-5.3%	-5.3%	-4.4%	-4.7%	-4.9%
Water Draw	0.0%	0.0%	0.0%	0.0%	0.0%	0.0%	0.0%	0.0%	0.0%	0.0%	0.0%
Preheat Tank Electrical Input	0.0%	0.0%	0.0%	0.0%	0.0%	0.0%	0.0%	0.0%	0.0%	0.0%	0.0%
Auxiliary Tank Electrical Input	-1.5%	-0.4%	1.7%	3.3%	-1.8%	-1.6%	-4.3%	3.1%	-0.6%	-2.1%	-0.2%
Total Electrical Input	-0.8%	-0.2%	0.6%	1.1%	-0.4%	-0.3%	-1.2%	0.6%	-0.1%	-0.6%	0.0%

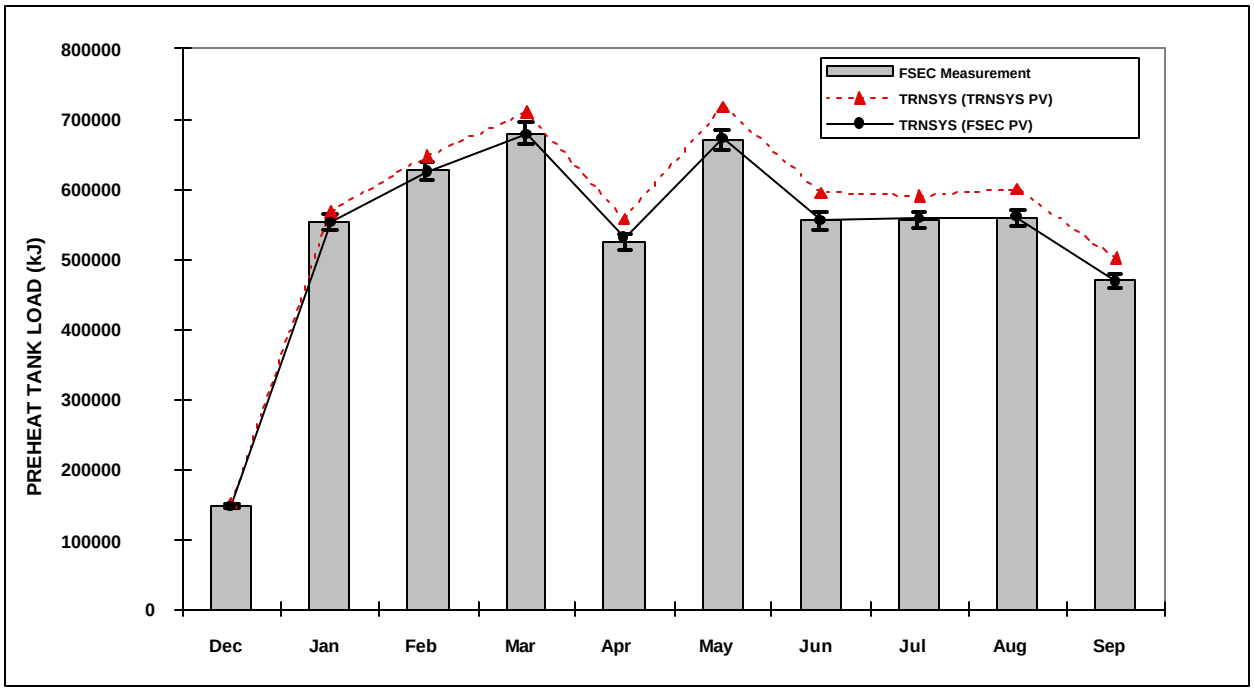

Figure 5.7.4.3-1 Measured and predicted monthly preheat tank water heating load. Predicted results with the electrical energy input determined by TRNSYS and measured by FSEC are shown. Error bars on experimental data are 2.3%.**{** TC **"Figure 5.7.4.3-1** Measured and predicted monthly preheat tank water heating load. Predicted results with the electrical energy input determined by TRNSYS and measured by FSEC are shown. Error bars on experimental data are 2.3%." **\l 5 }**

With the electrical energy input set by the FSEC measurements, the simulated total preheat tank load deviated from that measured by less than 0.1% for the period of this analysis. This discrepancy in tank load fell well within the approximate experimental uncertainty of ±2.3%. The average tank temperature determined by simulation was lower than measured by 1.4 C with the heat loss lower by 11.9%. The discrepancies in average tank temperature and heat loss were outside the approximate experimental uncertainty range of ±1.0 C and ±6.4%. The monthly preheat tank energy unbalances calculated from the measured data in Table 5.7.1-1 were about 1.4% of the total energy added to the tank and consistently less than zero. While this level of unbalance is less than the uncertainties in the components of the tank energy balance, it suggests that the unbalance was primarily the result of an overstatement of tank average temperature and heat

loss in the measurements. Monthly energy unbalances in the simulated results amounted to 0.07% of the total energy addition. No minutely tank temperature profile data were available for the FSEC system, but it is likely that the average tank temperature discrepancy noted here results from measurements of the bottom node temperature as was determined in the NIST simulation. The two prototypes were instrumented for measurements in an identical fashion.

5.7.4.4 The Auxiliary Tank Load and Heat Loss{ TC "5.7.4.4 The Auxiliary Tank Load and Heat Loss" \l 4 }

Tables 5.7.4.3-1 through 5.7.4.3-3 also show the results of simulating the FSEC auxiliary tank using the measured inlet water temperature during draws. Figure 5.7.4.4-1 shows the measured and predicted monthly auxiliary tank loads using the inlet water temperature determined by TRNSYS and that measured by FSEC.

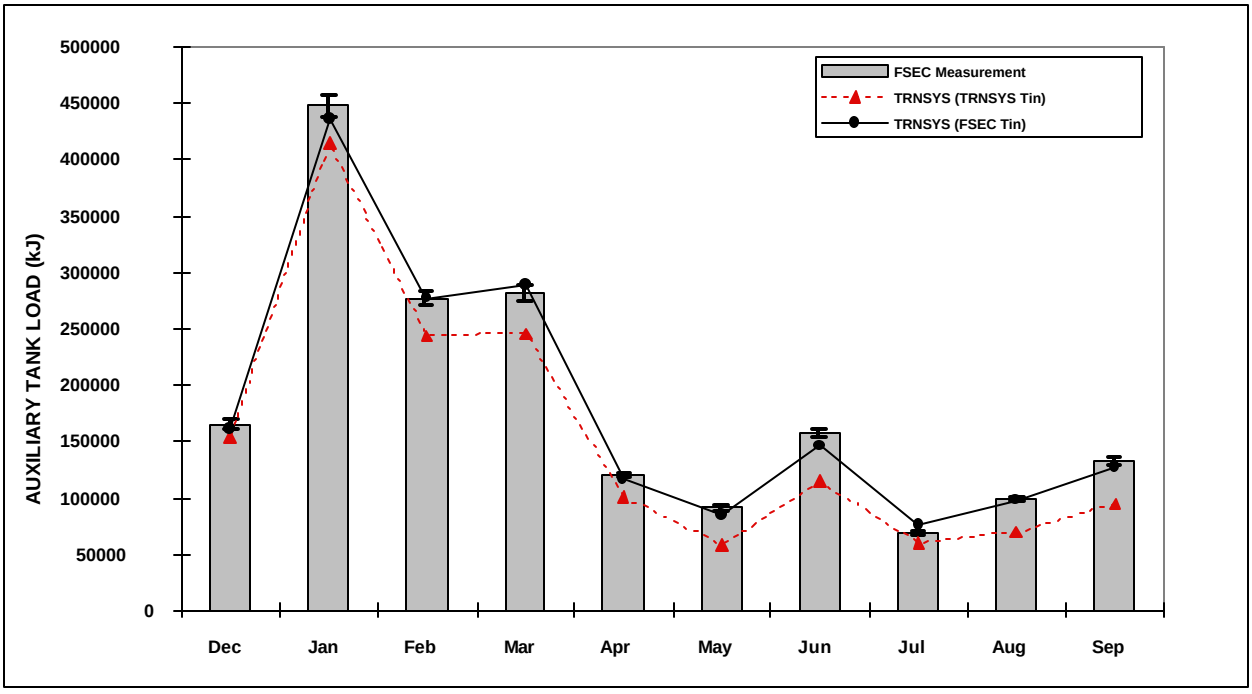

Figure 5.7.4.4-1 Measured and predicted monthly auxiliary tank water heating load. Predicted results with the inlet water temperature determined by TRNSYS and measured by NIST are shown. Error bars on experimental data are 2.3%.{ TC "**Figure 5.7.4.4-1** Measured and

predicted monthly auxiliary tank water heating load. Predicted results with the inlet water temperature determined by TRNSYS and measured by NIST are shown. Error bars on experimental data are 2.3%." \l 5 }

With thermostat setpoints of 51.3 C and 49.8 C used in modeling the original auxiliary tank and its replacement, respectively, the simulated electrical input to the tank was lower than that measured by 0.2% for the period of analysis. The model underpredicted the auxiliary tank load by 1.6% of the measured value for the nine month simulation period. The electrical energy input and load discrepancies fell within the approximate uncertainties in the measured results of ±1.0% and ±2.3%, respectively. The simulation predicted the average tank temperature and heat loss to be 2.0 C and 4.9% lower than measured (measurement uncertainties were ±1.0 C and ±6.4%, respectively). Much like in the case of the preheat tank, the monthly auxiliary tank energy unbalances from the measured data were consistently less than zero. The measured unbalances amounted to 2.7% of the total energy addition to the tank, greater than the uncertainties in the components of the energy balance. The tank analyses discussed previously would suggest that the measured unbalances resulted primarily from an overstatement of the average tank temperature and heat loss. The unbalances based on the simulated results were significantly smaller in magnitude (0.3% of the total energy added to the tank).

5.8 Conclusions{ TC "5.8 Conclusions" \l 2 }

With the exception of the significant overprediction of the PV array energy output in simulating the FSEC prototype, the TRNSYS model of a two-tank PV-SDHW system proved an excellent means of assessing the performance of such systems. For the purposes of this study, the results presented in this chapter were thought an adequate verification of the accuracy of the TRNSYS model.

The TRNSYS PV array model performed much better in comparison to experimental

results from NIST than those from FSEC. In the absence of additional PV array performance data from FSEC, beyond the energy output taken on an hourly basis during the operation of the PV-SDHW system, little can be learned about the discrepancy which occurred there with the model. If instantaneous current and voltage data for various loads and environmental conditions were available, perhaps the source of the difference in output could be discerned. The array model used in the TRNSYS simulations was determined by previous researchers (Townsend, 1989, Eckstein, 1990) to be a valid tool within reasonable bounds. When used in this study, the model compared favorably with an one experimental system and less favorably with another. The results of this study do not, however, suggest or warrant some important change in the model with the possible exception of the inclusion of some more sophisticated means of calculating array temperature.

The TRNSYS tank model agreed well with the measured results. During simulations in which the electrical input to the tanks was identical to the measured input (or nearly so in the case of the auxiliary tanks) and the inlet water temperature was exactly that measured, the TRNSYS tank model uniformly predicted average tank temperatures about 1.5 C below those measured. For various reasons, it was concluded that the measured tank temperatures and heat losses were overstated as discussed above. The tank model performed quite adequately for the purposes of this study.

With the TRNSYS PV-SDHW system model verified by comparison with experimental data, it was generalized in order to serve as a useful design and analysis tool. The following chapter describes this work.